

Alternative Splicing Results in Differential Expression, Activity, and Localization of the Two Forms of Arginyl-tRNA-Protein Transferase, a Component of the N-End Rule Pathway

YONG TAE KWON, ANNA S. KASHINA, AND ALEXANDER VARSHAVSKY*

Division of Biology, California Institute of Technology, Pasadena, California 91125

Received 13 August 1998/Returned for modification 21 September 1998/Accepted 6 October 1998

The N-end rule relates the *in vivo* half-life of a protein to the identity of its N-terminal residue. The underlying ubiquitin-dependent proteolytic system, called the N-end rule pathway, is organized hierarchically: N-terminal aspartate and glutamate (and also cysteine in metazoans) are secondary destabilizing residues, in that they function through their conjugation, by arginyl-tRNA-protein transferase (R-transferase), to arginine, a primary destabilizing residue. We isolated cDNA encoding the 516-residue mouse R-transferase, ATE1p, and found two species, termed *Ate1-1* and *Ate1-2*. The *Ate1* mRNAs are produced through a most unusual alternative splicing that retains one or the other of the two homologous 129-bp exons, which are adjacent in the mouse *Ate1* gene. Human *ATE1* also contains the alternative 129-bp exons, whereas the plant (*Arabidopsis thaliana*) and fly (*Drosophila melanogaster*) *Ate1* genes encode a single form of ATE1p. A fusion of ATE1-1p with green fluorescent protein (GFP) is present in both the nucleus and the cytosol, whereas ATE1-2p-GFP is exclusively cytosolic. Mouse ATE1-1p and ATE1-2p were examined by expressing them in *ate1*Δ *Saccharomyces cerevisiae* in the presence of test substrates that included Asp-βgal (β-galactosidase) and Cys-βgal. Both forms of the mouse R-transferase conferred instability on Asp-βgal (but not on Cys-βgal) through the arginylation of its N-terminal Asp, the ATE1-1p enzyme being more active than ATE1-2p. The ratio of *Ate1-1* to *Ate1-2* mRNA varies greatly among the mouse tissues; it is ~0.1 in the skeletal muscle, ~0.25 in the spleen, ~3.3 in the liver and brain, and ~10 in the testis, suggesting that the two R-transferases are functionally distinct.

The half-lives of intracellular proteins range from a few seconds to many days. The rates of processive proteolysis are a function of the cell's physiological state and are controlled differentially for specific proteins. In particular, most of the damaged or otherwise abnormal proteins are metabolically unstable. Many other proteins, while long-lived as components of larger macromolecular structures such as ribosomes and oligomeric proteins, are metabolically unstable as free subunits. Regulatory proteins are often also short-lived *in vivo*, providing a way to generate their spatial gradients and to rapidly adjust their concentrations, or subunit compositions, through changes in the rate of their synthesis or degradation (20, 23, 28, 39, 44, 55).

The posttranslational conjugation of arginine (Arg) to the N termini of eukaryotic proteins was described 35 years ago (26), but the function of this modification, and of the enzyme involved, Arg-tRNA-protein transferase (R-transferase) (47), remained unknown until the discovery that the identity of N-terminal residue in a protein influences its metabolic stability (4). The resulting relation was termed the N-end rule (54). Aspartate (Asp) and glutamate (Glu), the two N-terminal residues known to be arginylated by R-transferase (47), were shown to be destabilizing residues in the N-end rule (4). It was therefore proposed (4) that the function of R-transferase is to target proteins for degradation by conjugating Arg, one of the primary destabilizing residues, to secondary destabilizing N-terminal residues (Asp and Glu in fungi; Asp, Glu, and Cys in metazoans) (18) (Fig. 1). It was also proposed (4) that the analogous prokaryotic enzyme Leu, Phe-tRNA-protein transferase (L, F-transferase) (47) mediates the activity of N-termi-

nal Arg and Lys, which, in prokaryotes, would be the secondary destabilizing residues. These conjectures were confirmed (7, 17, 45, 53).

The similar but distinct degradation signals which together give rise to the N-end rule are called the N-degrons (54, 56). In eukaryotes, an N-degron comprises two determinants: a destabilizing N-terminal residue and an internal Lys residue of a substrate (5, 22). The Lys residue is the site of formation of a substrate-linked multiubiquitin chain (11). The N-end rule pathway is thus one pathway of the ubiquitin (Ub) system. Ub is a 76-residue protein whose covalent conjugation to other proteins plays a role in a multitude of processes, including cell growth, division, differentiation, and responses to stress (20, 23, 39, 55). In many of these processes, Ub acts through routes that involve the degradation of Ub-protein conjugates by the 26S proteasome, an ATP-dependent multisubunit protease (9, 13, 40, 43).

(In the text that follows, names of mouse genes are in italics, with the first letter uppercase. Names of human and *Saccharomyces cerevisiae* genes are also in italics, all uppercase. If human and mouse genes are named in the same sentence, the mouse gene notation is used. Names of *S. cerevisiae* proteins are roman, with the first letter uppercase and an extra lowercase "p" at the end. Names of the corresponding mouse and human proteins are the same, except that all letters but the last "p" are uppercase. The latter usage is a modification of the existing convention (50), to facilitate simultaneous discussions of yeast, mouse, and human proteins. In some citations, the abbreviated name of a species precedes the gene's name.)

The N-end rule is organized hierarchically. In the yeast *S. cerevisiae*, Asn and Gln are tertiary destabilizing N-terminal residues in that they function through their conversion, by the *NTAI*-encoded N-terminal amidase (Nt-amidase) (6), to the secondary destabilizing N-terminal residues Asp and Glu. The

* Corresponding author. Mailing address: Division of Biology, 147-75, Caltech, 1200 East California Blvd., Pasadena, CA 91125. Phone: (626) 395-3785. Fax: (626) 440-9821. E-mail: avarsh@cco.caltech.edu.

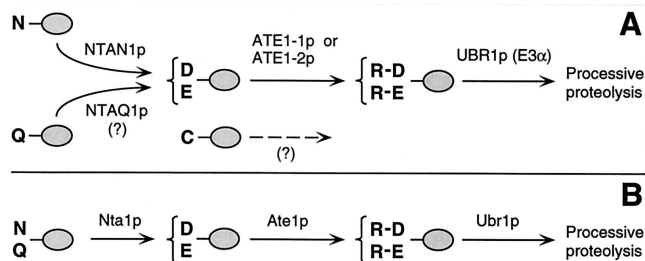


FIG. 1. Comparison of enzymatic reactions that underlie the activity of the tertiary and secondary destabilizing residues among eukaryotes. (A) Mammals (reference 54 and this work); (B) the yeast *S. cerevisiae* (5). N-terminal residues are indicated by single-letter abbreviations for amino acids; ovals denote the rest of a protein substrate. The *Ntan1*-encoded mammalian Nt-amidase converts N-terminal Asn to Asp, whereas N-terminal Gln is deamidated by a distinct Nt-amidase that remains to be identified (19, 51). In contrast, the yeast Nt-amidase can deamidate either N-terminal Asn or Gln (6). The secondary destabilizing residues Asp and Glu are arginylated by the mammalian ATE1-1p or ATE1-2p R-transferase (see Results). A Cys-specific mammalian R-transferase remains to be identified (see Results). N-terminal Arg, one of the primary destabilizing residues (54), is recognized by N-recogin (E3) (see the introduction).

destabilizing activity of N-terminal Asp and Glu requires their conjugation, by the *S. cerevisiae* ATE1-encoded Arg-tRNA-protein transferase (R-transferase), to Arg, one of the primary destabilizing residues (7) (Fig. 1B). In mammals, the deamidation step is bifurcated, in that two distinct Nt-amidases specific, respectively, for N-terminal Asn and Gln, mediate the activity of tertiary destabilizing residues (19, 51) (Fig. 1A). Mice lacking the Asn-specific Nt-amidase NTAN1p have recently been produced through targeted mutagenesis and found to be fertile, outwardly normal, but behaviorally distinct from their congenic wild-type counterparts (28a). In mammals, the set of secondary destabilizing residues contains not only Asp and Glu but also Cys, which is a stabilizing residue in yeast (18, 54) (Fig. 1).

The primary destabilizing N-terminal residues are bound directly by the UBR1-encoded N-recogin (also called E3 α), the recognition component of the N-end rule pathway (8). In *S. cerevisiae*, N-recogin is a 225-kDa protein that binds to potential N-end rule substrates through their primary destabilizing N-terminal residues, Phe, Leu, Trp, Tyr, Ile, Arg, Lys, and His (54). The *Ubr1* genes encoding mouse and human N-recogins, also called Ex (21, 41), have been cloned (29), and mouse strains lacking *Ubr1* have recently been constructed (29a).

The known functions of the N-end rule pathway include the control of peptide import in *S. cerevisiae*, through the degradation of Cup9p, a transcriptional repressor of *PTR2* which encodes the peptide transporter (2, 10); a role in regulating the Sln1p-dependent phosphorylation cascade that mediates osmoregulation in *S. cerevisiae* (38); the degradation of Gpa1p, a G α protein of *S. cerevisiae* (34); and the conditional degradation of alphaviral RNA polymerase in virus-infected metazoan cells (16, 54). Physiological N-end rule substrates were also identified among the proteins secreted into the host cell's cytosol by intracellular parasites such as the bacterium *Listeria monocytogenes* (46). Inhibition of the N-end rule pathway was reported to interfere with mammalian cell differentiation (24) and to delay limb regeneration in amphibians (52). Microarray-based comparisons of gene expression patterns in wild-type and congenic *ubr1 Δ strains of *S. cerevisiae* have shown that a number of yeast genes, of diverse functions, are significantly*

up- or down-regulated in the absence of the N-end rule pathway (39a).

The mammalian counterpart of the yeast ATE1-encoded R-transferase was partially purified from rabbit reticulocytes and shown to cofractionate with Arg-tRNA synthetase (12). Recent studies of the Ub-dependent proteolysis of endogenous proteins in muscle extracts suggested that the N-end rule pathway plays a major role in catabolic states that result in muscle atrophy (48, 49). A significant fraction of the N-end rule pathway's activity in muscle extracts was found to be tRNA dependent, indicating the involvement of R-transferase (48, 49). It was also reported that a crush injury to the rat sciatic nerve results in a ~10-fold increase in the rate of arginine conjugation to the N termini of unidentified proteins in the nerve's region upstream of the crush site (15, 57), suggesting an injury-induced increase in the concentration of R-transferase substrates and/or an enhanced activity of the N-end rule pathway.

In this work, we began the functional analysis of mammalian R-transferase (ATE1p) by isolating mouse cDNA encoding this enzyme. Surprisingly, we found two *Ate1* cDNA species, which were identical except for a 129-bp region that encoded similar but distinct sequences. One or the other, but not both, of the corresponding *Ate1* exons is retained in the mature *Ate1* mRNA, and the ratio of the resulting two species, *Ate1-1* and *Ate1-2*, varies greatly among mouse tissues. We also show that ATE1-1p and ATE1-2p, while differing in activity, can arginylate N-terminal Asp and Glu in model substrates. However, neither of them can arginylate N-terminal Cys, the known secondary destabilizing residue (18), suggesting the existence of a distinct Cys-specific mammalian R-transferase.

MATERIALS AND METHODS

Strains and plasmids. The *S. cerevisiae* strains used were JD55 (*MAT α ura3-52 his3- Δ 200 leu2-3,112 trp1- Δ 63 lys2-801 ubr1 Δ ::HIS3*) (34) and SGY3 (*MAT α ura3-52 lys2-801 ade2-101 trp1- Δ 63 his3- Δ 200 leu2- Δ ate1- Δ 2::LEU2*) (19a). Cells were grown in rich medium (YPD) or in synthetic media (SD) containing 0.67% yeast nitrogen base without amino acids (Difco), auxotrophic nutrients, and 2% glucose. To induce the P_{GAL} promoter, glucose was replaced by 2% galactose (SG medium). Transformation of *S. cerevisiae* was performed by the lithium acetate method (3).

The *ubr1* Δ *ate1* Δ double mutant AVY34 was constructed by replacing 93% of the ATE1 open reading frame (ORF) (the first 470 codons) in strain JD55 (*ubr1* Δ) by the *LEU2* gene, through homologous recombination (42) with the introduced *LEU2* gene flanked on either side by 40 bp of ATE1-specific sequences. Mutants were selected on SD (lacking Leu and His) plates, and Leu⁺ isolates were checked by PCR for the absence of ATE1 and by colony assays (7, 8) for the absence of Ate1p and Ubr1p activity. High-copy-number pUB23-X plasmids expressing Ub-X- β gal proteins (see below) from P_{GAL} in *S. cerevisiae* have been described elsewhere (4). Mouse *Ate1-1* and *Ate1-2* cDNAs (see below) were subcloned into the low-copy-number vector p414GAL1 (36), using the engineered *Bam*HI (5') and *Xho*I (3') restriction sites, yielding plasmids pAT1 and pAT2. For localization assays with green fluorescent protein (GFP), cDNAs encoding mouse ATE1-1p or ATE1-2p were subcloned into the pEGFP-N1 N-terminal protein fusion vector (Clontech, Palo Alto, Calif.), using the engineered *Xho*I (5') and *Age*I (3') restriction sites, yielding plasmids pAT1-GFP and pAT2-GFP.

Isolation of the mouse *Ate1-1* and *Ate1-2* cDNAs. The 392-bp fragment of the mouse EST (expressed sequence tag) clone (accession no. AA415294), which was identified in GenBank through species walking (see Results), was used as a probe to screen a λ gt10-based mouse cDNA library from MEL-C19 cells (Clontech), using standard procedures (3). Eight positive clones, whose inserts ranged from 0.5 to 1.6 kb, were analyzed by PCR and partial sequencing. The cDNA inserts of clones 3 and 8 were then subcloned into pBluescript II SK⁺ (29) and sequenced on both strands. The resulting ORFs were identical except for a 129-bp internal region (see Results) (Fig. 2A). The deduced amino acid sequences of the mouse cDNA clones 3 and 8 were weakly but significantly similar to the deduced sequences of *Caenorhabditis elegans* and *S. cerevisiae* ATE1p (see Results) (Fig. 2B) and corresponded to nucleotides (nt) 699 to 1870 and 587 to 2099, respectively, in the subsequently produced full-length mouse *Ate1-1* and *Ate1-2* cDNAs (accession no. AF079096 and AF079097).

A human EST clone (accession no. AA503372) whose deduced amino acid sequence was highly similar to that of the partial mouse *Ate1* cDNA clone 8 was found in GenBank, using the partial mouse ATE1p sequence as a query. This EST clone was purchased from Genome Systems (St. Louis, Mo.) and sequenced

A

Atel1 AAAAAATCCAAAAGGAGGAAACACAGAAAACATAAGCATAACTCCATCTGGTGTAGTAGTCTCTGACCCGAAAGGGCGGTAGCGGGCGGTGCGTAGGACTGGGTGGCGCAGGGCGGG 120
 Atel1 GGGTCGCGGACATGGCTTCTGGAGCGGCCTTCCACCTAGCCCTGTAGAGATTTTGGAGGCCAGACCTCTCCAGTGTGGCTACTGCAAGAACAGTGGCGACTGCGCTCATGGCA 240
 M A S W S A P S P S L V E Y F E G Q T S F Q G Y K N K L G S R S Y G M 37

Atel-2 TGTGGGCACATTCCATGACAGTGCAGGATATCAGGATCTTATAGACCGAGGATGGAGAAGAAGTGGGAAATATGTGTACAAACCTGTCATGGATCAAACTGCTGCTCAGTATACAA 360
 W A H S M T V Q D Y Q D L I D R G W R R S G K Y V Y K P V M D Q T P Q Y T I 77

Atel-2 TAAGGTGTACCTTTACAGTTTCAGCCATCAAAATCTCACAGAAAAGTTTGGAAAAAATGCTGAAATTTCTGGCTAAAGGAGAGATCTCGAAAGGCAATGTGAGGATGAGCCCATGG 480
 R C H P L Q F Q P S K S H K K V L K K M L K F L A K G E I S K G N C E D E P M D 117

Atel-2 ATTCTACAGTGGAGGATGCTGTTGACGGTACTTTGACATTAATAACAGCTGGATATAAGTGTGATCTCAAAACACTCAGTGCACCTAAAGGAAGCATAGAGAGTGAAGAGGAGA 600
 S T V E D A V D G D F A L I N K L D I K C D L K T L S D L K G S I E S E E K E K 157

Atel-2 AAGAAAAGATATAAAGAAAAGAGGCTTAAAGAATTCATCATCCACAATCTATAGAGGAGAAGTGGGGCTCTGGTGAACCATCACATCCAATCAAAGTTCATATTGGTCTCAAGCCAG 720
 E K S I K K E G S K E F I H P Q S I E E K L G S G E P S H P I K V H I G P K P G 197

Atel-2 GCAAAGGGGCTGACTTGAATAAGCCTCCATGTCGGAAAAGCAAGGAAATGAGGAAAAGAAAGCAAGATTAACACGGATCGACAGGCGCTCAGTGCAGCCTCGGAGGCTCAAGGTCAGC 840
 K G A D L S K P P C R K A R E M R K E R Q R L K R M Q Q A S A A S A Q A Q G Q P 237

Atel-2 -----V R I V P A S F
 -----GTGAGGCTGTACTGGCTCTCT
 Atel-1 CAGTCTGTTTGTACCAAGGCTAAATCCAACAGCCCAAGTCACTGGAAGATTTGATTTTCAATCTTTACCAGAAAATGCATCGCACAGTGTAGAGGTGAGGGTGGTAAGATCTCTC 960
 V C L L P K A K S N Q P K S L E D L I F Q S L P E N A S H K L E V R V V R S S P 277

Atel-2 E D P E N Q S P S L Y T K Y Q V A I H Q E A P E I C E K S E
 Atel-1 TTGAGGACCAGAGTTCACATCATCTTCAACAGTCTCTTCTTATATACCAAGTATCAAGTGGTATACACAGGAAAGCACCTGAAATATGTGAAAGTCTGAG----- 1080
 ACCAAGTCCCTCAGTTCAGAGCAGATTTACAGGCTTACACAGGCTTAAACAGCTACAGAGTGGTGTTCACAGGACCGCCCTCAAGCCAGTTCAGGCTTTACAGGATTC 317
 P S P Q P R A T E Q S Y Q V Y K R Y Q M V V H K D P P D K P T V S Q A Q G Q P

Atel-2 TTTCAGCTCACCATTGGAGGACAGACCCCTGCTGAGCCAGGATGAGTGGTGTGGCTCTTACCAGCAGTACTGGCTCGATGGGAGATCATGCTGTGGGGGTGTAGACATTC 1200
 C S S P L E A E H P A D G P E C G Y G S F H Q Q Y W L D G K T I A V G V L D I L 357

Atel-2 TCCCGTACTGTGTGTTTCTGTGTATCTACTACGATCTGATTTATTCATTTCTGTCTTGGGGTCTATTACGATTAAGAGAAATGCTTTTACTAGACAACCTGCATGAGAAAACAT 1320
 P Y C V F S V Y L Y D P D Y S F L S L G V Y S A L R E I A F T R Q L H E K T S 397

Atel-2 CGCACTCAGCTATTATATATGGGTTTCTACATTCCTCTCCCAAGTAGAGATACAGGGTCAATATAGACCTTCTGATTTGCTGTGCTGAGACGTATGCTGGGTGCCCATG 1440
 Q L S Y Y M G Y I H S C P K M R Y K G Q Y R P S D L L C P E T Y V W V L E 437

Atel-2 AGCAGTCCCTCTCTGAGCACTCCAAGTACTGCGGTTTCAACAGGACCCCGAAGCAGAGGATGAAGGACGCGAGTAAAGAACTTGACCCAGTAAAGGCTTTACAGAGGATCTG 1560
 Q C L F N S K Y C R F N Q D P E A E D E G R S K E L D R L R V F H R R S A 477
 C Q L P S L D N S L K Y C R F N Q D P E A E D E G R S K E L D R L R V F H R R S A

Atel-2 CCATGCTTACGCTGTTTATAAGAATCACCAAGAAGACCAAGTGGAGGCTGCTGTGTGGASTATGCAAACTCGTAGGACAGAAGTCTCGGAGAGGATGCTGCTGTTACAGACT 1680
 M P Y G V Y K N H Q E D P S E E A G V L E Y A N L V G Q K C S E R M L L F R H * 516

Atel-2 GAAGCCCTGACCTCAGCCAGCCGCGCCGCTGTCATCTTGGCAAGTCCACCTGCTCTGCTGCTGCGCCAGCTTCCACCAAGTACGTCAGGAGCTTTTAAAAATTTTGTGG 1800
 AATGATTTATGAGAACTTTGGTGTAAATATAAGATTTTAAAAATTTCTATGACCTAGCCCTTAAATGGGACTGTGCTTTGACGCTTCTTGGAGGCAAGGTTGCTTTCATGCT 1920
 CCAGTGAATTTTAGGGAAGAAAATGAAGAAGTCAATATAAGTCAATTTGTCCAGTACTGTCTGCTGCTGGAGAAATTTGACACAGAGACTGCTCTTTAGACCAATGGTCTTAA 2040
 CCTGGGGCTCACCACTCACAGGCCAATGTAGATAGCTGTGTGAGTCAACTCA 2099

B

Mm-Atel-1 MASWSAPSPSLVEYFEGQTSFQCGYCKNKL-GRSRYGMWAHS-----MTVVDY 47
 At-Atel1 MSLKNDASSHDGGSNRESVIDDHGRRKSTCGYCKSPARSSISHGLSAQT-----LTVVDY 56
 Dm-Atel1 MSLSIVSYGSOQSKCGYCGAGAN-CSLSHGMHAYQ-----LDCRDY 40
 Ce-Atel1 -----MTVVDY 6
 Sc-Atel1 MSDRFVIWAPSMHNPEAAKCGYCHGNKG GNMDDLFDLSWAHRYMNMKMDVVKIENCTIGSFVEHMDVATY 70

QDLDRCWRRSCKYVYKPVMDQTCPPQYTIIRCHPLQFOPSKSHKVKLKKMLKFLAKGEISKGNCEDEPMDSTVEDAVDGDFA L INKLDIKC 138
 QALDRGWRRSGTYLVKHEMDKTCPPYTIIRKASDVPVTKEQORVSRRLERFDGKLDVQPREORGASSGSDVSDTRRKTLAGAASEENKK 148
 QDLDRCWRRSCKYVYKPNQETCCPPYTIIRKNGLEFKLSKSNKRIILRRINRFL-----RDGKRESKPEAGDGEDAADYIVA----- 210
 SGLLDVGRWRRSGTYLVKLPDRVTCPPQYTIIRLDVTKKMSRSOKRAMRQMEFL-----ATGKRYPVCGIKEEPADPVENMLKG----- 83
 DRMCNMGFRRSCKFLYKVPDLRNCRCRYTIIRTAPELNMNTELKCKISRFASRIITSEDYCPAAVASSDFVGKIVNAEMN----- 149

DLKTLSDLKGSIESEEEKEKESIKKEGSKEFIHPQ-----SIEEKLGSGEPSHPIKVHIGPKPGKADLSKPPCRKAREMRKERORLKRMQ 225
 VEAVMDDLKNIDQAVQLCIRSGEFPSPNMQIPKASVKKVFCARRKKLAEGTEQILYTSINAFPIAAAIKRIQTSEKIGNSAEGNRLSPETI 240
 -----PEVTAS-EPQPLPKSPPVINVEQVASLA-----TAQRKPTKQA TAAVEAPT LGSNKSAAPISNKPCKAKOMRLDRRLAKLGD 201
 -----SGSQSEOSKKNLKSHEVSTKK-----MKDADRPVLTKKEIRNKKFEEK-----ROKNLDPDVPTERRQK 144

ASAAASEAQGPVCLLPKAKS-----NQPSLEDLIFQSLPENASHKLEVRVRRSSPPSPQFRA 284
 SEMLLSAMHKVGETPDVSIKCYKGHINFLSSAKDSFSDRDVVPNGNISRGANSLDQSEILHAKKDNSENHQARKKLEIHLKRSSFDPEE-- 329
 ASYSTKSLT-----QEKTLRDF-LNTDSETNKHRKLRLI--HVDDEFR 244
 DAA-----RQRTIQSYIDEARPDW-KHKLEKLV--SLGDFEFG 181
 -----SKFTYTRFEPALYSEK----- 166

TFQESYQVYKRYQMVVHKDPPDKPTVSQFTFLCSSPLEAHPADGPE-----CGYGSFHQQYVLDGKIIVAVGVLDILPY 359
 -----HELKRYQLKLVHNDKPGHVVESSYRFLVDSPLIDVQPSGDEKVPV-----CGFGSFHQQYRIDGRILAVGVVDILPK 402
 TLPQSFALYKQYQISIHNDPPKQD--DAYKEHLQATPLQNEKPDGPE-----MGYGSFHQQYVLDGKIIVAVGVVDILPK 317
 RDNESFELYKNYOHIIHKDQDCL--AGFRFLCDSPILKKERGG-----TELGSFHLLDGLAVGVVDILPK 251
 -----YHLEVKYQEKVHODYNNSP--KSFKRFLCDTDFGPEAVLGTQESWEQLNNWORMKPGKELKHMGPVHECYYYEGLIATVSDILPS 251

CVFSVYLYDPDYSFLSLGVTYSAALREIAFTRQLHEKTSQLSYYVNGEYIHSCKMRYKQGYRPSDILCPETVYVWPVIEQCLPSLD---(73 aa) 516
 CLSSVYLFVDPDYAFSLSLGKYSATQELNWIENQARCPSLQYYVLYGYIHSCKMRYKAAAYRPSLCLCPLRFQWVPEVARPMLD---(143 aa) 629
 CVSSVYFFVDPDYAFSLSLGKYSALREIEQLVQSLAEKVPSLKYYVNGEYIHSCKMRYKQGLRPSDILCPETVYVWPLTDVIRAKL---(76 aa) 477
 CFSAKYMYNPEYSFLSLGVTYALREIEQTLRHAIYSNLKYYVNGEYIHSCKMRYKAKFRPSDILCDQSFVWDFNSCRDLLD---(81 aa) 416
 GISVYFVDPDYFKWSLGLSALRDLAIIGR-----TNLQYYVLYGYIEDCPKMYKANYGAEVLDVCHSKYIPLKPIODMISR---(173 aa) 503

identity / similarity

C

		Y Q	H	M8	M3
Mm-Atel-1	V R V V R S S P P S P Q F F R A T F Q E S Y Q V Y K R Y Q M V V H K D P P D K P T V S Q				33 / 61
Hs-Atel-1	V R V V R S S P P S S Q F F K A T T L L E S Y Q V Y T K R Y Q M V V I H K N P P D T P T E S Q			81 / 91	30 / 58
Mm-Atel-2	V R V V P A S F E D P E F F N S S F N Q S S P S L Y V T K Y Q V A I H Q E A P E I C E K S E			33 / 61	
Hs-Atel-2	V R L V P V S F E D P E F F K S S F S Q S S P S L Y V T K Y Q V A I H Q D P P D E C G K T E			37 / 61	77 / 86
Dm-Atel	L R L I - - H V Y D D E F R R T L P Q S S F A L Y K K Y Q Q H I T H N D P P K D Q D A Y K			33 / 64	42 / 61
Ce-Atel	L K L V - - L G G D E F F E F F T R D N E S F E L Y K K Y Q Q H I T H K D E D C R L A G - -			33 / 56	44 / 62
At-Atel	I H L K R S S F D P E F F - - - - - H E L Y K K R Y Q D L K V H N D K P G H V V E S S			41 / 62	31 / 57
Sp-Atel	V T M E P C T Y T D E K - - - - - F E V F K K Y Q M Q V H L E K E E I T K K G			33 / 60	31 / 54
Sc-Atel	T R F E P A L Y S E E K - - - - - Y H L F V K Y Q M E K V H Q D Y N N S P K S - -			30 / 57	33 / 64

to obtain more of the 5'-proximal human *ATE1* sequence. Reverse transcription-PCR (RT-PCR) (3) was then carried out with poly(A)⁺ RNA from mouse embryonic fibroblasts, using the mouse *Ate1*-specific reverse primer 5'-CCTTTGGTAACAACAGACTGGCTG-3' and the forward primer 5'-TCTCATAGACCGAGGATGGCGAAG-3', whose sequence was derived from the above human EST clone. The resulting PCR products, which appeared as a smear upon agarose gel electrophoresis, were ligated into the TA cloning vector (Invitrogen, San Diego, Calif.), and the ligation mixture was used as a template for PCR using a nested mouse *Ate1* primer 5'-CTGCAGCTGAGGCCTGCTGCATCCG-3' and a vector-specific primer 5'-GTTTTCCAGTCACGAC-3'. This strategy yielded a single major DNA species (data not shown). We then applied 5'-RACE (rapid amplification of 5' cDNA ends) (3), using the above RT-PCR-derived sequence, to produce the full-length *Ate1* cDNA as previously described (19).

Analysis of the mouse *Ate1* gene. The mouse genomic DNA from L cells was used as a template for PCR, using the Expand high-fidelity PCR system (Boehringer, Indianapolis, Ind.) and exon-specific primers as previously described (29), to produce DNA fragments that together spanned ~4 kb of the mouse *Ate1* gene and contained the two alternative 129-bp *Ate1* exons. The regions encompassing exon/intron junctions were sequenced by using exon- and intron-specific primers. Thereafter, a strategy described earlier for the *Ubr1* gene (29) was used to screen, using a fragment of the mouse *Ate1* cDNA (nt 255-1139), a BAC (bacterial artificial chromosome)-based library of mouse genomic DNA fragments from strain 129SvJ (Genome Systems), yielding one BAC clone containing the mouse *Ate1* gene.

Isolation of the human, plant, and fly *ATE1* cDNAs. Using the cloned mouse *ATE1p* sequences (see above) as queries, we identified in GenBank several significantly similar EST sequences from other organisms (data not shown). To determine whether these species also contained the two forms of *ATE1* mRNA, we isolated the corresponding *ATE1* cDNAs. RT-PCR (3) with poly(A)⁺ RNA from human 293 cells and the primers 5'-CAATGGCATGTGGGCACATTCATG-3' (specific for the human EST clone AA503372 [see above]) and 5'-CCACAGGTACTGAATATGTATCCTG-3' (specific for the human EST clone AA195361) was carried out, yielding a 1.6-kb human *ATE1* cDNA fragment lacking the first 41 codons of the *ATE1* ORF. This fragment (a mixture of the two alternative cDNAs) was subcloned into the TA vector (Invitrogen) and sequenced on both strands. Full-length *Ate1* cDNAs from *Arabidopsis thaliana* and *Drosophila melanogaster* were isolated by RT-PCR as well, using total RNA from *A. thaliana* leaves, poly(A)⁺ RNA from *D. melanogaster* embryos, and primers specific for the 5' and 3' ends of the corresponding ORFs. By using the strategy described above for the human *ATE1* cDNAs, the sequences of these primers were derived from the EST clones that were initially identified in GenBank through their similarity to the mouse *ATE1p* sequence, then purchased from Genome Systems, and sequenced prior to RT-PCR with the corresponding RNA preparations. The final human, plant, and fly *ATE1* cDNAs were sequenced on both strands.

Assays of β -gal. Colony assays for the *Escherichia coli* β -galactosidase (β gal) in *S. cerevisiae* were carried out by overlaying yeast colonies on SG plates with 0.5% agarose containing 0.1% sodium dodecyl sulfate (SDS), 4% dimethylformamide, and a 0.1-mg/ml solution of the chromogenic β gal substrate X-Gal (5-bromo-4-chloro-3-indolyl- β -D-galactopyranoside; Calbiochem, La Jolla, Calif.), followed by incubation for 1 to 2 h at 37°C. Quantitative assays for β gal in *S. cerevisiae* were carried out with whole-cell extracts, using another chromogenic β gal substrate, *o*-nitrophenyl- β -D-galactopyranoside (ONPG). Cells in a 5-ml culture (A_{600} of ~1) were pelleted by centrifugation and resuspended in 5 ml of buffer Z (60 mM Na₂HPO₄, 40 mM NaH₂PO₄, 10 mM KCl, 1 mM MgSO₄, 50 mM β -mercaptoethanol [pH 7.0]). After the A_{600} of the suspension was determined 50- or 100- μ l samples were diluted to 1 ml with buffer Z; 0.1% SDS (20 μ l) and CHCl₃ (50 μ l) were then added; the suspension was vortexed for 10 to 15 s and incubated for 15 min at 30°C, followed by the addition of 200 μ l of ONPG (4 mg/ml in buffer Z) and further incubation at 30°C, until a medium yellow color had developed, at which point the reaction was stopped by the addition of 1 M Na₂CO₃ (0.4 ml). The mixture was centrifuged for 5 min at 1,100 \times g, and the A_{420} and A_{500} of the samples were measured. The ONPG units

(U_{ONPG}) of β gal activity were calculated as follows: $U_{ONPG} = 1,000 \times [(A_{420}) - (1.75 \times A_{500})] / t \times v \times A_{600}$, where t and v were, respectively, the time of incubation (minutes) and the sample volume (milliliters) (3).

Purification and N-terminal sequencing of X- β gal proteins. Extracts were prepared (using the liquid nitrogen procedure [3]) from *S. cerevisiae* AVY34 (*ubr1 Δ ate1 Δ*) cotransformed with a pUB23-X plasmid (4) (expressing Ub-X- β gal) and either pAT1 (expressing mouse *ATE1-1p*) or pAT2 (expressing mouse *ATE1-2p*). Cultures were grown in SG to an A_{600} of ~1. Specific X- β gal proteins (X = Asp or Cys) were purified by affinity chromatography on ProtoSorb lacZ (Promega, Madison, Wis.), a monoclonal anti- β gal antibody coupled to agarose beads (Promega). X- β gal proteins were further purified by electrophoresis on SDS-7% polyacrylamide gels and were electroblotted onto Immobilon-P^{SO} membranes (Millipore, Bedford, Mass.). N-terminal sequencing of 10 to 15 pmol of electroblotted X- β gal was carried out for at least five cycles, using an Applied Biosystems 476A protein sequencer (Caltech Microchemistry Facility).

Mouse cell cultures, transfection, and GFP localization. NIH 3T3 cells (ATCC 1658-CRL) were grown as monolayers in Dulbecco's modified Eagle medium (GIBCO, Frederick, Md.) supplemented with 10% fetal bovine serum. Cells for GFP localization analyses were grown to ~15% confluence on glass coverslips for 24 h prior to transfection with either pAT1-GFP or pAT2-GFP, using Lipofectamine (GIBCO) and the manufacturer-supplied protocol. Cells were incubated for 5 h at 37°C in serum-free medium containing DNA and Lipofectamine. Thereafter an equal volume of medium containing 20% serum was added, and the cells were grown for another 12 to 20 h at 37°C. Cells were fixed with 2% formaldehyde in phosphate-buffered saline, and GFP fluorescence was visualized in a Zeiss Axiophot microscope.

Northern hybridization. Mouse multiple-tissue Northern blots containing 2 μ g of poly(A)⁺ RNA per lane (Clontech) were probed with the ³²P-labeled 1.1-kb mouse *Ate1* cDNA (nt 638 to 1734), using the manufacturer-supplied protocol.

Determination of the relative levels of *Ate1-1* and *Ate1-2* mRNAs. Samples of total RNA isolated as described previously (3) from mouse spleen, skeletal muscle, liver, brain, testis, and embryonic fibroblasts were subjected to RT-PCR (28 cycles). The primers 5'-CAGTGGAGGATGCTGTTGACGGTGAC-3' and 5'-GTGCTCTGCCCAATGGTGAGCTG-3' were specific for the identical regions of *Ate1-1* and *Ate1-2* cDNAs that flanked the two 129-bp exons (see Results) which distinguished these cDNAs. The resulting 624-bp product (a mixture of the *Ate1-1* and *Ate1-2* cDNA fragments) was treated with *ScrFI*, which cuts at different sites within the two 129-bp exons, followed by a 2% agarose gel electrophoresis. This procedure made it possible to distinguish the *Ate1-1* and *Ate1-2* fragments. The ratios of the two forms of *Ate1* cDNA were determined by serial dilutions of the samples prior to gel electrophoresis.

Nucleotide sequence accession numbers. The nucleotide sequences reported in this paper were submitted to the GenBank/EMBL data bank and assigned accession no. AF079096 (mouse *Ate1-1* cDNA), AF079097 (mouse *Ate1-2* cDNA), AF079098 (human *Ate1-1* cDNA), AF079099 (human *Ate1-2* cDNA), AF079100 (*A. thaliana* *Ate1* cDNA), and AF079101 (*D. melanogaster* *Ate1* cDNA).

RESULTS

Identification of mouse *Ate1* cDNAs by species walking. On the assumption that the sequences of R-transferases in different species might be sufficiently conserved to be detected by using the sequence of the only cloned R-transferase, *S. cerevisiae* *Ate1p* (7), we have been searching GenBank and related databases. No mammalian sequences in GenBank, including the EST sequences, had significant similarities to *S. cerevisiae* *Ate1p*. However, we did identify a nematode (*C. elegans*) ORF (accession no. Z21146) that exhibited similarity to yeast *Ate1p* (Fig. 2B) and then used the *C. elegans* sequence to identify a

FIG. 2. Two forms of the mouse *Ate1* cDNA and the ATE protein family. (A) The mouse *Ate1-1* and *Ate1-2* cDNAs and their products. The nucleotide sequences of *Ate1-2* identical to those of *Ate1-1* (everywhere except for the 129-bp region) are indicated by dashes. In the region of the alternative 129-bp exons of *Ate1-1* and *Ate1-2*, white-on-black and gray shadings highlight, respectively, identical and similar residues. The circled Cys residues are homologous to those that are important for the enzymatic activity of *S. cerevisiae* *Ate1p* (32). (B) The ATE protein family and the origins of the alternative 129-bp exons. Alignment of the sequences of mouse *ATE1-1p* (Mm-*Ate1-1*), *A. thaliana* *Ate1p* (At-*Ate1*), *D. melanogaster* *Ate1p* (Dm-*Ate1*), *C. elegans* *Ate1p* (Ce-*Ate1*), and *S. cerevisiae* *Ate1p* (Sc-*Ate1*) (accession no. J05404). Similar residues (gray) were grouped as follows: M, L, I, and V; D, E, N, and Q; R, K, and H; Y, F, and W; S, A, and T. The region encoded by the alternative 129-bp exons of mouse *Ate1* is highlighted by a thick line. Of the Cys residues that are conserved among all ATE proteins, the ones required and not required for the enzymatic activity of *S. cerevisiae* *Ate1p* (32) are indicated, respectively, by \blacktriangledown and ∇ . The N-terminally truncated mouse *ATE1-1p* and *ATE1-2p* proteins which began at Met-42 (\bullet) lacked the R-transferase activity (data not shown). The highly variable C-terminal regions of ATE proteins were omitted from the alignment. The sequences were aligned using PileUp program (Wisconsin Package; Genetics Computer Group, Madison, Wis.). Gaps (-) were introduced to optimize the alignment. The residue numbers are on the right of the sequences. The sequence of *C. elegans* *Ate1p* appears to lack the N-terminal region of other ATE proteins because of an error in defining the *Ate1* ORF in the genomic DNA sequence (accession no. Z21146). (C) Alignment of the 43-residue regions that are encoded by the alternative 129-bp exons in mammalian *Ate1*. Sequences shown: mouse (Mm-*Ate1-1* and Mm-*Ate1-2*), human (Hs-*Ate1-1* and Hs-*Ate1-2*), *D. melanogaster* (Dm-*Ate1*), *C. elegans* (Ce-*Ate1*), *A. thaliana* (At-*Ate1*), *S. pombe* (Sp-*Ate1*; accession no. Z99568), and *S. cerevisiae* (Sc-*Ate1*) (accession no. J05404). The degrees of identity and similarity of ATE proteins to the deduced amino acid sequences of the M8 (mouse *ATE1-1p*) or M3 (mouse *ATE1-2p*) exon of the mouse *Ate1* gene are indicated on the right. The residues conserved among all of the compared sequences are indicated above the alignment.

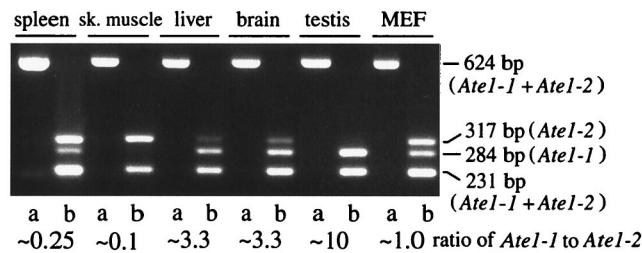


FIG. 3. Expression of *Ate1-1* and *Ate1-2* mRNAs in different mouse tissues and mouse embryonic fibroblasts (MEF). Two forms of *Ate1* cDNA (Fig. 2A) were amplified in a single reaction by RT-PCR, using the same primers, to yield 624-bp fragments that included the region of the alternative 129-bp exons (see Materials and Methods). The 624-bp fragments were digested with *ScrFI*, which produced a 231-bp fragment (a mixture of *Ate1-1* and *Ate1-2*), a 284-bp, *Ate1-1*-specific fragment, and a 317-bp, *Ate1-2*-specific fragment. The untreated (lanes a) and *ScrFI*-treated (lanes b) samples from different mouse tissues were analyzed by electrophoresis in a 2% agarose gel. The ratio of the two forms of *Ate1* mRNA, defined as the ratio of the 284-bp (*Ate1-1*) fragment to the 317-bp (*Ate1-2*) fragment, was determined by analyzing serially diluted samples and comparing the resulting band intensities (data not shown). sk., skeletal.

significantly similar EST sequence of *D. melanogaster* cDNA (accession no. AA391570). Finally, using the deduced amino acid sequence of the *Drosophila* EST clone as a probe, we identified a 467-bp mouse EST sequence (accession no. AA415294) that exhibited weak but significant similarity to the *Drosophila* sequence but no detectable similarity to *S. cerevisiae* Ate1p. On a chance that this 467-bp EST had been derived from the mouse *Ate1* cDNA, we used it to screen a mouse cDNA library and indeed isolated the putative mouse *Ate1* cDNAs (Fig. 2A).

Alternative splicing results in two species of mouse *Ate1* cDNA containing distinct but homologous exons. During the initial mouse cDNA library screening, we found that the cDNA clone 3 (nt 699 to 1870 of *Ate1-2* cDNA) was identical to the cDNA clone 8 (nt 587 to 2099 of *Ate1-1* cDNA), except for a 129-bp region whose deduced amino acid sequences were similar (31% identity; 61% similarity) (Fig. 2). The two full-length *Ate1* cDNAs (termed *Ate1-1* and *Ate1-2*), which were obtained by RT-PCR followed by 5'-RACE (see Materials and Methods), encoded proteins of identical length, 516 residues (59.2 kDa and pI of 8.14 versus 59.1 kDa and pI of 7.22) (Fig. 2A), that contained regions of similarity to the 57.8-kDa Ate1p of *S. cerevisiae* (Fig. 2B). RT-PCR (followed by subcloning) with RNAs from different mouse tissues also produced the two forms of *Ate1* cDNAs, indicating that the two species were in fact present in the initial RNA preparation (Fig. 3 and data not shown).

To determine whether both of the two 129-bp regions of the *Ate1-1* and *Ate1-2* cDNAs were a part of the *Ate1* gene, and whether *Ate1-1* and *Ate1-2* were produced through alternative splicing, we analyzed the mouse *Ate1* gene in the vicinity of its two 129-bp exons, using at first PCR and subsequently a BAC clone containing *Ate1* (see Materials and Methods). The two 129-bp exons were located next to each other in the *Ate1* gene (Fig. 4A). We also found that the 12-bp sequences around the splice acceptor sites of these exons (6 bp in the intron and 6 bp in the exon) were identical between the two exons (Fig. 4B), consistent with the alternative presence of these exons in the mature *Ate1* mRNA. The exon-containing RT-PCR products from different mouse tissues appeared as a single major band retaining one of the two 129-bp exons (Fig. 3 and data not shown). Subcloning and analyses of these RT-PCR products yielded no other differentially spliced *Ate1* cDNAs (for example, cDNAs retaining both or neither of the two 129-bp exons),

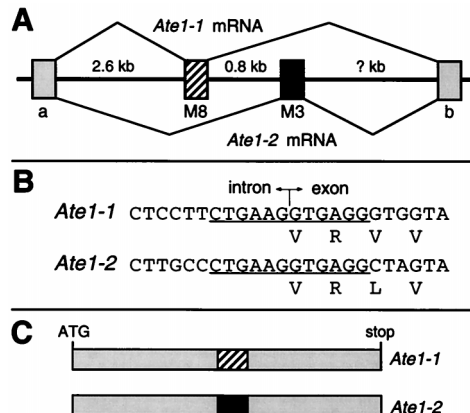


FIG. 4. The two forms of mouse *Ate1* mRNA are produced by alternative splicing. (A) The two alternative 129-bp exons are adjacent in the mouse *Ate1* gene. The thick line denotes genomic DNA; the striped and black rectangles denote the alternative 129-bp exons, M8 and M3 (see Materials and Methods); gray rectangles denote the flanking *Ate1* exons, of unknown sizes; thin lines denote the alternative splicing patterns that yield the two forms of *Ate1* mRNA. (B) The underlined 12 bp (6 bp in the intron and 6 bp in the exon) around the splice acceptor sites are identical between the two alternative 129-bp exons. (C) Scale diagrams of the two forms of mouse *Ate1* cDNAs. The alternative 129-bp exons M8 and M3 are indicated by the striped and black boxes, respectively.

suggesting that the splicing of *Ate1* pre-mRNA is tightly regulated to retain one and only one of the two alternative exons. Thus, the two forms of *Ate1* mRNAs are produced by a nearly unprecedented (see Discussion) splicing pathway which ultimately yields two proteins of identical size that bear two alternative, homologous but distinct 43-residue internal sequences (Fig. 4C).

The absence of alternative 129-bp exons from the plant and fly *Ate1* genes. To explore the evolution of *Ate1*, and especially the phylogeny of its alternative 129-bp exons, we cloned the human, plant (*A. thaliana*), and fly (*D. melanogaster*) *ATE1* cDNAs (see Materials and Methods). Two forms of the human *ATE1* cDNA, termed *Hs-ATE1-1* and *Hs-ATE1-2*, were isolated from human 293 cells (the forms' molar ratio was about 1). However, only one form of the *Ate1* cDNA was isolated from either the leaves of *A. thaliana* (termed *At-Ate1*) or *D. melanogaster* embryos (termed *Dm-Ate1*), suggesting that the alternative 129-bp exons may not be present in the *Ate1* genes of plants and arthropods. The *A. thaliana* and *D. melanogaster* Ate1p proteins were, respectively, 629 and 477 residues long (71 and 55 kDa, with pIs of 6.0 and 8.4). Mouse ATE1-1p was 82, 38, and 42% identical (as well as 91, 57, and 61% similar) to human ATE1-1p, *A. thaliana* Ate1p, and *D. melanogaster* Ate1p, respectively (Fig. 2 and data not shown). *A. thaliana* Ate1p bore a 16-residue region containing exclusively Asp or Glu (data not shown).

We used RT-PCR and RNA preparations from *A. thaliana* and *D. melanogaster* to amplify the relevant regions of the corresponding *Ate1* cDNAs. The resulting fragments were digested with restriction enzymes that recognize, in each species, exclusively the region that corresponds to the 129-bp exons of the mouse *Ate1* cDNAs, and the products were analyzed by gel electrophoresis. The initial cDNA fragments of *A. thaliana* and *D. melanogaster* *Ate1* completely disappeared after this treatment, in contrast to the homologous mouse cDNA fragment (which contained two distinct sequences of identical length), suggesting that the two alternative exons were absent from the *Ate1* genes of plants and arthropods (Fig. 5A).

While this analysis was under way, complete sequences of

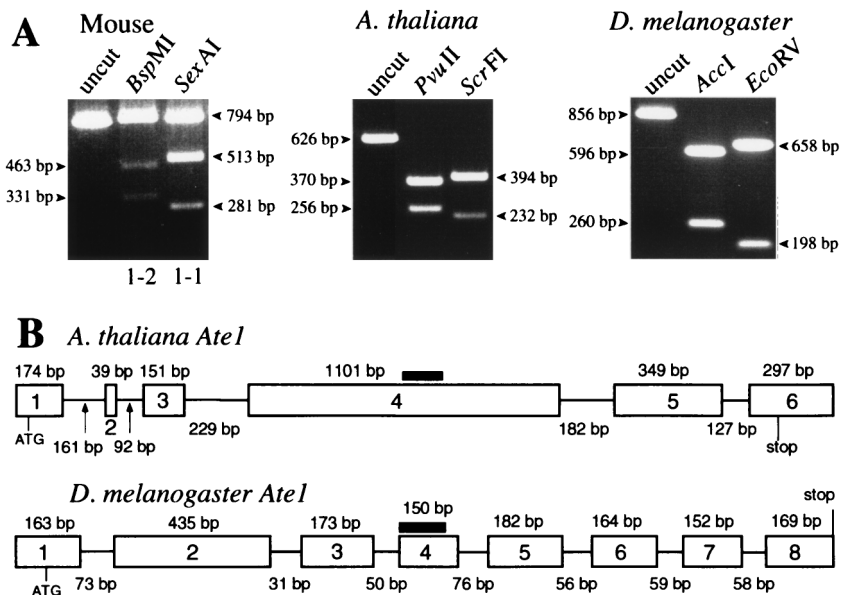


FIG. 5. Alternative splicing of *Ate1* pre-mRNA in mammals (the mouse) but in neither plants (*A. thaliana*) nor arthropods (*D. melanogaster*). (A) The relevant *Ate1* cDNA fragments from mouse (794 bp), *A. thaliana* (626 bp), and *D. melanogaster* (856 bp) were produced by RT-PCR (see Materials and Methods). The products were treated with the indicated restriction endonucleases that cut exclusively within the two alternative 129-bp exons of mouse *Ate1* cDNAs (*Bsp*MI for *Ate1-2*; *Sex*AI for *Ate1-1*) or within the corresponding regions of *A. thaliana* (*Pvu*II and *Scr*FI) and *D. melanogaster* (*Acc*I and *Eco*RV) *Ate1* cDNAs. (B) The *A. thaliana* and *D. melanogaster* *Ate1* genes. The exon-intron organization of these genes was deduced through comparisons of their cDNA sequences, determined in this work (see Materials and Methods), with the concurrently determined sequences of the corresponding genomic DNA regions (see text). The horizontal lines and rectangles denote, respectively, introns and exons, whose lengths are indicated below and above the line denoting introns. Thick horizontal lines indicate the regions of *A. thaliana* and *D. melanogaster* cDNAs that correspond to the alternative 129-bp exons of the mouse and human *Ate1* cDNAs (Fig. 2 and 4). The lengths of the *A. thaliana* and *D. melanogaster* *Ate1* genes are, respectively, ~3 and ~2.5 kb.

the *A. thaliana* and *D. melanogaster* *Ate1* loci, determined through the corresponding sequencing projects, were deposited in GenBank (accession no. AA005237 and accession no. AC004321, respectively). By comparing the cloned *Ate1* cDNAs (see Materials and Methods) and the corresponding genomic sequences of *A. thaliana* and *D. melanogaster*, we could deduce the organization of these *Ate1* genes. The results (Fig. 5B) directly confirmed the absence of the alternative homologous exons from *Ate1* of *A. thaliana* and *D. melanogaster*, in contrast to mammalian *Ate1*. The corresponding region of plant *Ate1p* is more similar to the exon-encoded sequence of mouse ATE1-1p, whereas in *Drosophila* this region is more similar to the alternative sequence of ATE1-2p (Fig. 2C). The corresponding regions of *S. cerevisiae* and *Schizosaccharomyces pombe* *Ate1p* are not preferentially similar to either of the two alternative exon-encoding sequences of mouse ATE1p (Fig. 2C).

Mouse ATE1-1p and ATE1-2p can implement the Asp/Glu-specific subset of the N-end rule pathway but differ in activity.

To determine whether the two putative mouse R-transferases are in fact R-transferases and to compare their activities in vivo setting, we examined whether ATE1-1p and ATE1-2p could confer metabolic instability on Asp- β gal and Glu- β gal in *ate1* Δ *S. cerevisiae*. Asp and Glu are secondary destabilizing residues in the N-end rule (Fig. 1 and introduction). The test substrates Asp- β gal and Glu- β gal (produced through cotranslational deubiquitylation of Ub-Asp- β gal and Ub-Glu- β gal (4)) are short-lived in wild-type yeast (half-lives of ~3 and ~30 min, respectively) but long-lived (half-life of >20 h) in *ate1* Δ *S. cerevisiae* that lacks the ATE1-encoded yeast R-transferase (5, 7). Previous work (19, 33) has shown that the steady-state level of an X- β gal protein is a sensitive measure of its metabolic stability.

S. cerevisiae *ate1* Δ cells were cotransformed with a pair of

plasmids that expressed one of the two putative mouse R-transferases, ATE1-1p or ATE1-2p, and one of several test substrates (as the corresponding Ub fusions): Asp- β gal, Glu- β gal, Arg- β gal, Cys- β gal, or Met- β gal. Met and Cys are stabilizing residues in the yeast N-end rule; Arg is a primary destabilizing residue; Asp and Glu are secondary destabilizing residues (5, 56). Control tests included either the vector alone or a plasmid expressing *S. cerevisiae* Ate1p. The steady-state levels of X- β gal proteins were determined by measuring the enzymatic activity of β gal in yeast extracts. Using this assay, we found that both forms of mouse ATE1p were able to confer metabolic instability on either Asp- β gal or Glu- β gal in *ate1* Δ *S. cerevisiae* (Fig. 6A). ATE1-1p and ATE1-2p destabilized Glu- β gal much less than Asp- β gal (Fig. 6A), consistent with Glu being a less destabilizing residue in the N-end rule than Asp, presumably because of less efficient arginylation of the N-terminal Glu by R-transferases (54). However, while the apparent destabilizing activity of the mouse ATE1-1p R-transferase was only slightly lower than that of *S. cerevisiae* Ate1p (expressed from the identical vector and promoter), the activity of mouse ATE1-2p was significantly lower than that of ATE1-1p (Fig. 6A).

We also asked whether the two forms of mouse ATE1p could influence each other's activity if they were coexpressed in the same cell (such an influence might be expected, for instance, if the active form of R-transferase were a dimer or if the two forms of R-transferase competed for binding to the same component of a pathway). *S. cerevisiae* *ate1* Δ cells were cotransformed with two plasmids bearing different selectable markers and expressing different combinations of ATE1-1p and ATE1-2p (1+1, 2+2, or 1+2), and also with a plasmid expressing one of the X- β gal test proteins (X = Met, Arg, Cys, Asp, or Glu). Control cells were cotransformed with the two

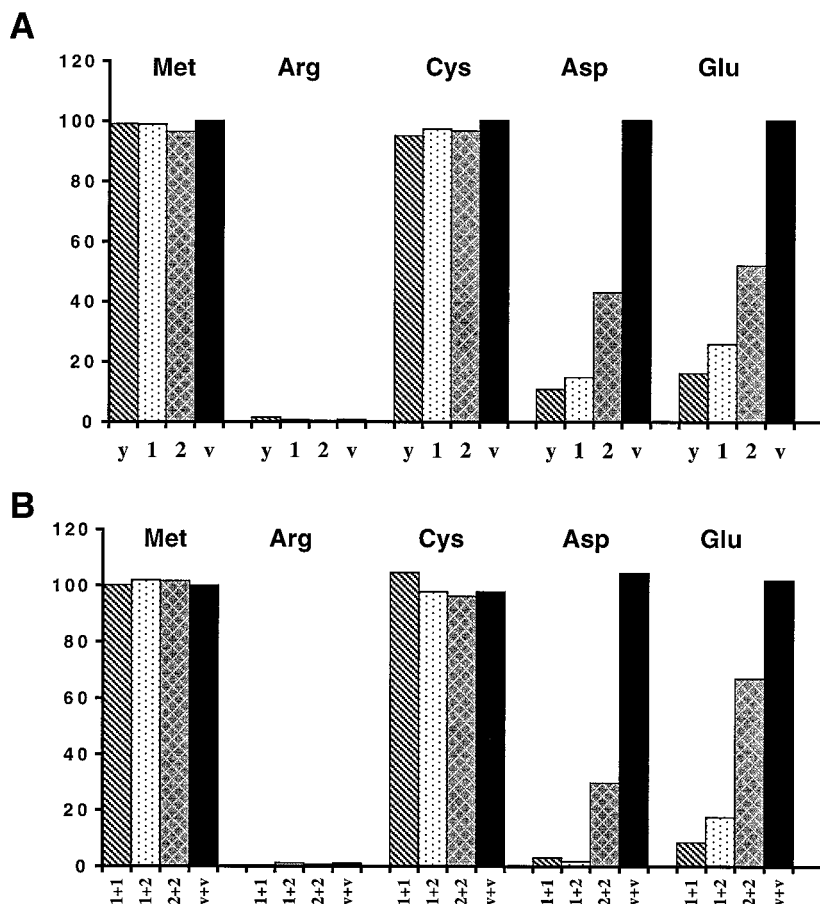


FIG. 6. The two forms of mouse ATE1p can implement the Asp/Glu-specific subset of the N-end rule pathway. (A) Relative enzymatic activities of β gal in *ate1 Δ* *S. cerevisiae* transformed with plasmids expressing X- β gal (as Ub-X- β gal) test proteins (X = Met, Arg, Cys, Asp, or Glu) together with a plasmid expressing either yeast ATE1 (denoted as y), mouse ATE1-1p (denoted as 1), mouse ATE1-2p (denoted as 2), or the vector alone (denoted as v). The N-terminal residues of X- β gals in each set of experiments are indicated at the top. The activity of Met- β gal in cells transformed with vector alone is taken as 100%. (B) The two forms of mouse ATE1p exhibit no cooperativity in mediating the degradation of X- β gals. Shown are relative enzymatic activities of X- β gals in *ate1 Δ* *S. cerevisiae* strain cotransformed with plasmids expressing X- β gals (Ub-X- β gals) (X = Met, Arg, Cys, Asp, or Glu) and the combinations of plasmids expressing the following proteins: mouse ATE1-1p and ATE1-1p (1+1), ATE1-1p and ATE1-2p (1+2), ATE1-2p and ATE1-2p (2+2), or two vector controls (v+v). One of the two vectors bore the *TRP1* marker and the other bore the *HIS3* marker (see Materials and Methods). Results are averages of four independent measurements, which differed by less than 10%.

vectors alone. The results (Fig. 6B) indicated that the total activities of the 1+1 and 1+2 combinations (measured as the extent of destabilization of Asp- β gal or Glu- β gal) were similar to each other and much higher than the total activities of 2+2 (Fig. 6B), consistent with the conjecture that the two forms of mouse R-transferase do not interact and that ATE1-1p is a more (possibly much more) active enzyme than ATE1-2p.

Neither ATE1-1p nor ATE1-2p confers metabolic instability on Cys- β gal. Cysteine is a stabilizing residue in the yeast N-end rule but a secondary destabilizing residue in multicellular organisms such as mammals and amphibians (14, 18, 30, 54). The presence of two alternative regions in the two forms of mouse R-transferase (Fig. 4C) initially suggested that one R-transferase might be specific for N-terminal Asp and Glu, with the other specific for Cys. However, Cys- β gal, which is long-lived in wild-type *S. cerevisiae* (5), remained long-lived in the presence of either ATE1-1p or ATE1-2p (Fig. 6A). This finding and, more directly, the results of amino acid sequencing (see below) suggest the existence of a mammalian tRNA-dependent enzyme (presumably a distinct R-transferase) (18) that mediates destabilizing activity of N-terminal Cys.

Mouse ATE1-1p and ATE1-2p destabilize Asp- β gal and Glu- β gal through arginylation of their N-terminal residues.

To verify directly that mouse ATE1-1p and ATE1-2p in fact possess the R-transferase activity, we constructed the *ate1 Δ ubr1 Δ* *S. cerevisiae* double mutant AVY34, which lacked both R-transferase and N-recognin (E3), the main recognition component of the N-end rule pathway (see Materials and Methods). Consequently, N-terminal arginylation of a test protein in this mutant by an exogenous R-transferase would not result in degradation of the protein, thereby making it possible to isolate enough of the test protein for N-terminal sequencing. Strain AVY34 was transformed with pUB23-D (expressing Ub-Asp- β gal) and also with either pAT1 (expressing ATE1-1p), pAT2 (expressing ATE1-2p), or vector alone and was grown in SG medium. Asp- β gal proteins isolated from these transformants were subjected to N-terminal sequencing (see Materials and Methods). The results (Table 1) directly confirmed that both ATE1-1p and ATE1-2p possessed R-transferase activity. In agreement with the finding that ATE1-1p was more active than ATE1-2p in destabilizing Asp- β gal in vivo (Fig. 6A), Asp- β gal from cells expressing ATE1-1p was

TABLE 1. N-terminal sequencing of X- β gal proteins isolated from *ate1 Δ ubr1 Δ S. cerevisiae* expressing different R-transferases

Substrate	Coexpressed protein	N-terminal sequence	Yield (%)
D-e ^K - β gal	Vector alone	D-H-G-S-A-	~100
D-e ^K - β gal	Mouse ATE1-1p	D-H-G-S-A-	~100
D-e ^K - β gal	Mouse ATE1-2p	R-D-H-G-S-A-	~50
D-e ^K - β gal	Mouse ATE1-2p	D-H-G-S-A-	~50
C-e ^K - β gal	Vector alone	C-H-G-S-A-	~20
C-e ^K - β gal	Mouse ATE1-1p	C-H-G-S-A-	~20
C-e ^K - β gal	Mouse ATE1-2p	C-H-G-S-A-	~20

found to be completely arginylated, whereas Asp- β gal from cells expressing ATE1-2p was arginylated to approximately 50% (Table 1).

We also determined, using the above procedure, whether mouse ATE1-1p or ATE1-2p could arginylate N-terminal Cys. Approximately 80% of Cys- β gal isolated from *ate1 Δ ubr1 Δ S. cerevisiae* was found to be N-terminally blocked, presumably acetylated (Table 1). However, the rest of Cys- β gal (~20%) bore the N-terminal sequence beginning with Cys and lacking N-terminal Arg, in agreement with the results of the *in vivo* Cys- β gal degradation assays (Fig. 6 and Table 1). Thus, both ATE1-1p and Ate1-2p are apparently unable to utilize N-terminal Cys as a substrate in *S. cerevisiae*.

ATE1-2p is exclusively cytosolic, whereas ATE1-1p is present in either the nucleus or the cytosol. To determine the intracellular location of the two forms of mouse R-transferase,

we constructed fusions to the N terminus of GFP and transiently expressed them in NIH 3T3 cells. Whereas the free 26-kDa GFP was located in both the nucleus and the cytosol (data not shown), the 85-kDa Ate1-2p-GFP fusion was exclusively cytosolic in all of the many transfected cells examined (Fig. 7a to c). In contrast, the 85-kDa ATE1-1p-GFP (the alternative form of R-transferase that is much more active enzymatically than ATE1-2p) was found to be localized differently in different cells on the same coverslip, possibly depending on their cell cycle position and/or metabolic state. Specifically, in ~50% of the transfected cells, ATE1-1p-GFP was exclusively cytosolic (Fig. 7d and e), as was ATE1-2p-GFP (Fig. 7a to c), but in the other ~50% of cells, ATE1-1p-GFP was present in the nucleus as well and, moreover, appeared to be significantly enriched in the nucleus (Fig. 7f and g). Thus, the two 43-residue alternative regions in ATE1-1p and ATE1-2p confer overlapping but nonidentical intracellular distributions on the respective R-transferases.

While the nonuniformity of the ATE1-1p-GFP localization among mouse cells in a single culture remains to be understood, its preferential location in the nuclei of some cells is consistent with a high content of basic residues in its 43-residue region, in comparison to the alternative homologous region of ATE1-2p (Fig. 2C). (No sequences fitting the consensus sequences of known nuclear localization signals could be detected in the 43-residue region of ATE1-1p). In contrast to mouse R-transferases, *S. cerevisiae* Ate1p was shown to be located predominantly in the nuclei of yeast cells (56a).

The ratio of *Ate1-1* to *Ate1-2* mRNA varies greatly among mouse tissues. Northern hybridization, using the 1.1-kb mouse *Ate1* cDNA fragment (nt 638 to 1734) as a probe, detected a

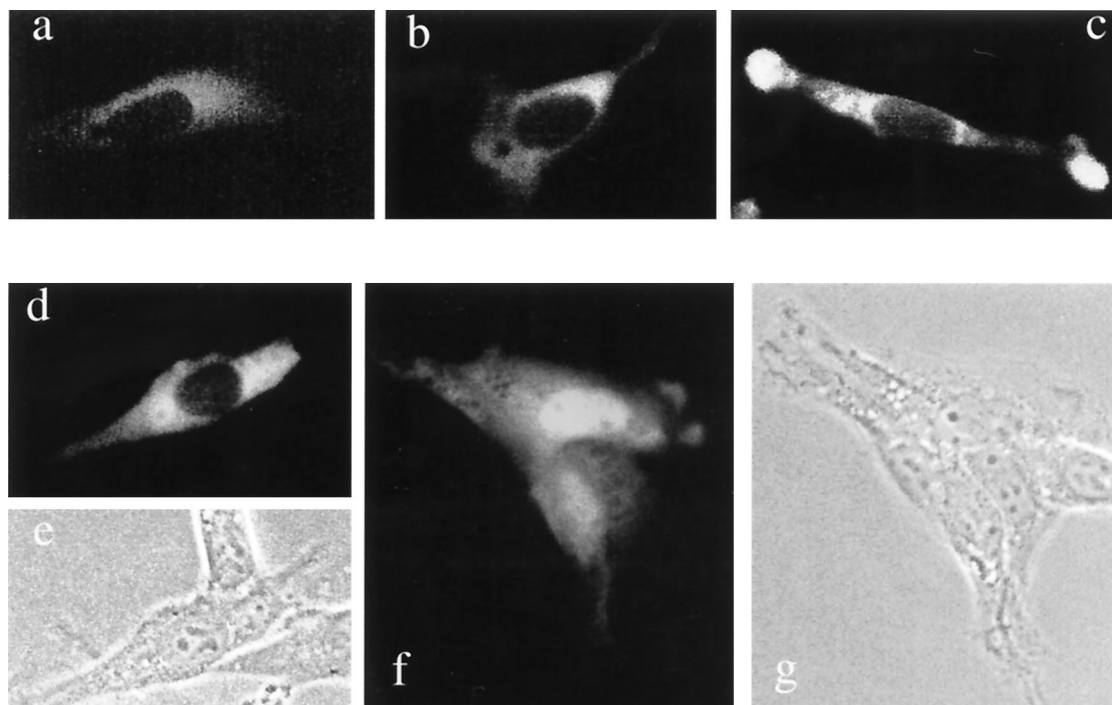


FIG. 7. Intracellular localization of mouse ATE1-1p and ATE1-2p. Shown are green (GFP) fluorescence (a to d and f) and phase-contrast (e and g) micrographs of mouse NIH 3T3 cells transiently transfected with ATE1-1p-GFP (d to g) or ATE1-2p-GFP (a to c) fusion proteins (see Materials and Methods). Panels a to c show different examples of the exclusively cytosolic localization of ATE1-2p. Regions around the nucleus and in the lamellar protrusions at the edges of a cell (c) exhibit higher GFP fluorescence, possibly because of a greater thickness of cells in these areas. Panels d plus e and f plus g show pairs of GFP fluorescence and phase-contrast pictures of cells that express ATE1-1p-GFP. The cell in panels d and e shows ATE1-1p-GFP in the cytosol but not in the nucleus. Cells in panels f and g contain ATE1-1p-GFP in both the cytosol and the nucleus, the latter being apparently enriched in ATE1-1p-GFP.

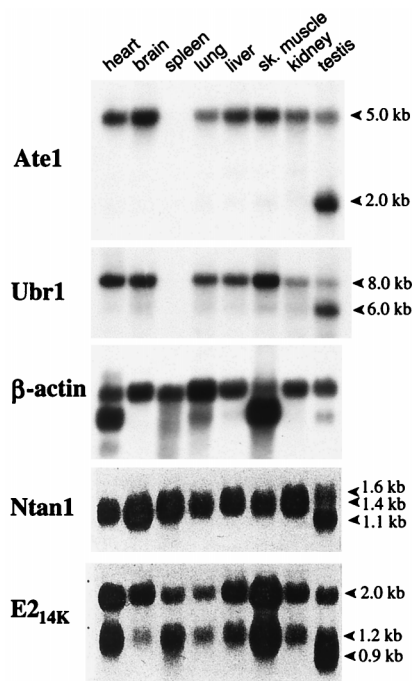


FIG. 8. Northern hybridization analyses of mouse *Ate1* mRNA. The Northern blots of mRNA from different mouse tissues were probed with an *Ate1* cDNA fragment (nt 638 to 1734) which can hybridize to both forms of *Ate1* mRNA. A mouse β -actin cDNA probe was used for comparing the total RNA loads as described previously (19). The same blot was also hybridized with mouse *Ubr1* (29) (see the introduction). The apparent absence of *Ate1* and *Ubr1* mRNAs from the spleen is an artifact of RNA degradation in this lane of the blot (data not shown). Also shown are the results of analogous Northern hybridizations of the mouse *Ntan1* cDNA, encoding the Asn-specific Nt-amidase (Fig. 1A), and *E2_{14K}*, encoding the relevant Ub-conjugating (E2) enzyme (19). The approximate sizes of transcripts are indicated on the right.

single ~5.0-kb transcript (a mixture of the *Ate1-1* and *Ate1-2* mRNAs) in all of the mouse tissues examined except the testis, where the ~5-kb *Ate1* mRNA was a minor one, the major species being ~2 kb (Fig. 8). Both ATE1p and the other targeting components of the mammalian N-end rule pathway are expressed ubiquitously (at various levels), and the testis-specific patterns of transcripts are characteristic for all of them as well (Fig. 8). The existence of the Y-chromosome-encoded, testis-specific variant of the Ub-activating (E1) enzyme (27, 35) suggests that the testis-specific modifications of the N-end rule pathway may be functionally relevant in spermatogenesis.

To determine the ratio of *Ate1-1* to *Ate1-2* mRNA in different mouse tissues or cells in culture, we employed RT-PCR, using sequence differences between the two alternative, homologous 129-bp exons to distinguish between them (see Materials and Methods) (Fig. 3). Approximately equal amounts of *Ate1-1* and *Ate1-2* mRNAs were present in mouse embryonic fibroblasts and in human 293 cells in culture (Fig. 3 and data not shown). However, the molar ratio of *Ate1-1* to *Ate1-2* mRNA was found to vary greatly among the mouse tissues: it was ~0.1 in the skeletal muscle, ~0.25 in the spleen, ~3.3 in the liver, and brain, and ~10 in the testis (Fig. 3). Thus, while the total expression of *Ate1* (*Ate1-1* plus *Ate1-2*) varies by 2- to 4-fold among mouse tissues (Fig. 8), the difference in expression levels between *Ate1-1* and *Ate1-2* mRNAs can be as high as a 100-fold (the skeletal muscle versus the testis) (Fig. 3), suggesting that the two forms of R-transferase may be functionally distinct.

DISCUSSION

The N-end rule pathway is one of several proteolytic pathways of the Ub system (23, 54, 55). Among the targets of the N-end rule pathway are proteins that bear destabilizing N-terminal residues. In the yeast *S. cerevisiae*, Asn and Gln are tertiary destabilizing N-terminal residues in that they function through their conversion, by a specific amidase (6), to the secondary destabilizing N-terminal residues Asp and Glu. The destabilizing activity of N-terminal Asp and Glu requires their conjugation, by the *ATE1*-encoded R-transferase, to Arg, one of the primary destabilizing residues (7) (Fig. 1B). In mammals, the set of secondary destabilizing residues contains not only Asp and Glu but also Cys, which is a stabilizing residue in yeast (18, 54) (Fig. 1).

In this work, we isolated cDNA encoding the mouse R-transferase, ATE1p, and found that this enzyme exists in two forms, termed ATE1-1p and ATE1-2p, which differ by containing one of the two alternative, homologous 43-residue regions. The two 516-residue R-transferases are produced from the mouse *Ate1* gene by a pathway of alternative splicing that retains one or the other of the two homologous 129-bp exons. The presence of two adjacent, homologous, equal-length, and alternatively utilized exons in a gene (Fig. 4) is nearly unprecedented. To our knowledge, just one such case was described previously: the mouse κ E2 enhancer-binding protein E12/E47 (37). The two κ E2-binding proteins, E12 and E47, are produced through a switch between two alternative, equal-length exons, resulting in two helix-loop-helix DNA-binding proteins that differ in the ability to homodimerize. Specifically, E47 can bind to the κ E2 enhancer either as a homodimer or as a heterodimer with MyoD, whereas E12 can bind as a heterodimer with MyoD but not as a homodimer (37).

We report the following major findings.

(i) Identification, through species walking, and isolation of the mouse cDNA encoding R-transferase (or ATE1p) have shown that mammalian ATE1p exists in two forms, ATE1-1p and ATE1-2p, which differ exclusively by one of the two alternative, homologous 43-residue regions (Fig. 2A).

(ii) The corresponding alternative 129-bp exons are adjacent in the mouse *Ate1* gene. Moreover, the 12-bp sequences around the splice acceptor sites of these exons (6 bp in the intron and 6 bp in the exon) are identical between the two exons (Fig. 4). The splicing of *Ate1* pre-mRNA proceeds in such way that one, and only one, of the alternative 129-bp exons is always retained in the mature *Ate1* mRNA.

(iii) The human *ATE1* gene also contains the two alternative 129-bp exons, whereas the plant (*A. thaliana*) and fly (*D. melanogaster*) *Ate1* genes encode a single form of ATE1p (Fig. 2 and 5). The corresponding 43-residue regions are significantly similar among all of the sequenced R-transferases, from *S. cerevisiae* to mammals (Fig. 2C). The set of *Ate1* genes from mammals to yeast defines a distinct family of proteins, the ATE family. The splicing-derived alternative forms of R-transferase have evolved apparently after the divergence of the arthropod and vertebrate lineages.

(iv) Expression of the mouse *Ate1-1* and *Ate1-2* cDNAs in *ate1 Δ* *S. cerevisiae*, and N-terminal sequencing of isolated X-gal test proteins, was used to show that ATE1-1p and ATE1-2p could implement the Asp/Glu-specific subset of the N-end rule pathway and that they did so through the arginylation of N-terminal Asp or Glu in the test substrates (Fig. 6A and Table 1).

(v) While the destabilizing activity of the mouse ATE1-1p R-transferase is only slightly lower than that of *S. cerevisiae* R-transferase, the activity of mouse ATE1-2p is significantly

(possibly considerably) lower than that of ATE1-1p. This conclusion follows also from a comparison of the N-terminal arginylation of Asp- β gal by the two R-transferases (Table 1). The results of coexpressing mouse ATE1-1p and ATE1-2p in the same *ate1 Δ* yeast cells were consistent with the conjecture that R-transferase functions as a monomer (Fig. 6B).

(vi) Neither ATE1-1p nor ATE1-2p could confer instability on (or arginylate) Cys- β gal in *ate1 Δ* *S. cerevisiae* (Fig. 6A and Table 1). Cys is a stabilizing residue in yeast but a secondary destabilizing residue in the mammalian N-end rule (54). A distinct Cys-specific mammalian R-transferase suggested by these data remains to be identified.

(vii) Mouse ATE1-2p (tested as a GFP fusion) was exclusively cytosolic in mouse 3T3 cells, whereas ATE1-1p was localized differentially in different cells of the same (unsynchronized) culture: it was either exclusively cytosolic or present in both the cytosol and the nucleus (Fig. 7).

(viii) Mouse *Ate1* is a ubiquitously expressed gene. A single ~5-kb mRNA was present in all of the tissues examined except the testis, where the major *Ate1* transcript was ~2 kb in length (Fig. 8). The testis-specific differential expression patterns are also characteristic of the other targeting components of the mammalian N-end rule pathway, such as the *Ntan1*-encoded Asn-specific Nt-amidase and the *Ubr1*-encoded N-recognin (E3 α) (19, 29).

(ix) The molar ratio of *Ate1-1* to *Ate1-2* mRNA varies up to a 100-fold among different mouse tissues (Fig. 3 and Results), suggesting a functional significance of the difference between the two R-transferases.

The region of ATE1p that corresponds to the two 129-bp mammalian *Ate1* exons has been significantly conserved throughout eukaryotic evolution, Tyr-296, Gln-297, and His-301 of the mouse ATE1-1p being among the most highly conserved residues (Fig. 2C). No putative members of the ATE family could be detected among the currently known prokaryotic ORFs. The most highly conserved region of R-transferases is an 82-residue stretch (residues 336 to 417) of mouse ATE1p: this region is 95, 76, and 63% identical to the corresponding regions of the human, *D. melanogaster*, and *A. thaliana* ATE1p, respectively (Fig. 2B). A Cys residue(s) is likely to be a component of the active site of R-transferase (31, 32). Among the five fully conserved Cys residues in proteins of the ATE family, four are located in the 56-residue N-terminal region (residues 23 to 78 of mouse ATE1p) (Fig. 2B). Conversion of some of these cysteines in *S. cerevisiae* Ate1p to alanines was found to decrease greatly the R-transferase activity of yeast Ate1p (16a, 32). Furthermore, derivatives of mouse ATE1-1p and ATE1-2p that lacked the first 42 residues were completely inactive in the yeast-based Asp- β gal degradation assay of a kind described in Fig. 7 (data not shown). Finally, a 90-residue C-terminal truncation of *S. cerevisiae* Ate1p did not result in a major decrease of its R-transferase activity (16a). Thus, the active site of R-transferase is likely to encompass at least some of the above N-terminal cysteines.

Since the two mammalian R-transferases (Fig. 4C) are identical in size and, except for a 43-residue region, are identical otherwise as well, it is likely that the previously described (partially purified) mammalian R-transferases (12, 47) were in fact mixtures of Ate1-1p and Ate1-2p. On the other hand, fractionation of a crude R-transferase preparation from rabbit reticulocytes did yield, in addition to a major fraction of R-transferase, chromatographically distinct R-transferase fractions that were not investigated further (12). The ratio of Ate1-1p to Ate1-2p in rabbit reticulocytes is currently unknown.

A splicing-mediated switch that replaces the 129-bp *Ate1*

exon of ATE1-1p with the alternative 129-bp exon results in a protein, ATE1-2p, that has a significantly (possibly considerably) lower R-transferase activity (Fig. 6). In addition, ATE1-2p is unable to enter the nucleus (as a GFP fusion), in contrast to ATE1-1p (Fig. 7). Taken together with the finding that the expression ratio of the two *Ate1* mRNAs, *Ate1-1* and *Ate1-2*, varies up to a 100-fold among different mouse tissues (Fig. 3 and Results), these data suggest that the two R-transferases are functionally distinct as well. Cited below are some of the possibilities that are consistent with the available evidence.

Mouse ATE1-2p has the R-transferase activity but arginylates, at steady state, only ~50% of Asp- β gal in *ate1 Δ* *S. cerevisiae*, in contrast to both ATE1-2p and *S. cerevisiae* Ate1p (Fig. 6 and Table 1). Moreover, the inefficient arginylation by ATE1-2p occurs in spite of its overexpression in *S. cerevisiae*. In contrast, the yeast Ate1p, which in wild-type *S. cerevisiae* is a weakly expressed protein (7), can quantitatively arginylate in vivo an overexpressed substrate such as Asp- β gal (18). Thus, at a low level of expression (which is likely to be the case in the mouse), the ATE1-2p R-transferase may be, in effect, an inactive enzyme, in contrast to ATE1-1p. If so, ATE1-2p might act as an (indirect) inhibitor of the ATE1-1p function, for example, through a competition with ATE1-1p for the binding to a component of the targeting complex in the N-end rule pathway. (The apparent absence of such competition in *S. cerevisiae* [Fig. 6B] may result from the lack of binding by ATE1p to heterologous yeast proteins.) It is also possible that a large difference in activity between mouse ATE1-1p and ATE1-2p in yeast reflects not their different enzymatic activities in the mouse but a (physiologically irrelevant) differential recognition of an essential yeast cofactor such as Arg-tRNA. Direct comparisons of arginylation kinetics by the purified mouse and yeast R-transferases will be required to address this unlikely but unexcluded interpretation.

Another possibility is that ATE1-2p has a distinct enzymatic activity that has been missed by the current N-terminal arginylation assay (Fig. 6 and Table 1). For example, ATE1-2p might be able to arginylate an internal residue in a substrate protein. In vitro enzymological dissection of ATE1-1p and ATE1-2p will address this and related conjectures. Yet another possibility is that the alternative 43-residue regions of ATE1-1p and ATE1-2p confer different metabolic stabilities on the two R-transferases, the lower apparent activity of ATE1-2p in yeast being due at least in part to its shorter half-life. A test of this model in mouse cells requires antibodies specific for the alternative regions of the two R-transferases; preparation of such antibodies is under way.

In yeast, the N-end rule pathway is present in both the cytosol and the nucleus. The apparent exclusion of mouse ATE1-2p from the nucleus and the different ratios of *Ate1-1* to *Ate1-2* mRNA among the mouse tissues suggest that the rule book of the N-end rule pathway may be regulated differentially in the cytosol and the nucleus, through a cell-type-specific expression of the pathway's components that are located in one but not the other compartment.

Physiological substrates for either eukaryotic R-transferases (54) or their prokaryotic counterparts, L, F-transferases (1, 25, 45) are not known. The cloning and characterization of the first mammalian *Ate1* cDNAs and genes (Fig. 2), and the discovery of alternative splicing that yields mouse ATE1-1p and ATE1-2p (Fig. 4) should facilitate understanding of the functions of mammalian R-transferases, in part through the analysis of ATE1-1p and ATE1-2p enzymes and also because it is now possible to construct mouse strains that lack ATE1-1p and/or ATE1-2p.

ACKNOWLEDGMENTS

The first two authors contributed equally to this work.

We thank Gary Hathaway of the Caltech Microchemistry Facility for the sequencing of X- β gal proteins. We are grateful to Hai Rao, Glenn Turner, Fangyong Du, and Lawrence Peck for helpful suggestions and to Fangyong Du, Federico Navarro-Garcia, Hai Rao, and Youming Xie for comments on the manuscript.

This work was supported by grants DK39520 and GM31530 to A.V. from the National Institutes of Health.

REFERENCES

- Abramochkin, G., and T. E. Shrader. 1995. The leucyl/phenylalanyl-tRNA-protein transferase. Overexpression and characterization of substrate recognition, domain structure, and secondary structure. *J. Biol. Chem.* **270**:20621–20628.
- Alagramam, K., F. Naider, and J. M. Becker. 1995. A recognition component of the ubiquitin system is required for peptide transport in *Saccharomyces cerevisiae*. *Mol. Microbiol.* **15**:225–234.
- Ausubel, F. M., R. Brent, R. E. Kingston, D. D. Moore, J. A. Smith, J. G. Seidman, and K. Struhl (ed.). 1996. *Current protocols in molecular biology*. Wiley-Interscience, New York, N.Y.
- Bachmair, A., D. Finley, and A. Varshavsky. 1986. *In vivo* half-life of a protein is a function of its amino-terminal residue. *Science* **234**:179–186.
- Bachmair, A., and A. Varshavsky. 1989. The degradation signal in a short-lived protein. *Cell* **56**:1019–1032.
- Baker, R. T., and A. Varshavsky. 1995. Yeast N-terminal amidase: a new enzyme and component of the N-end rule pathway. *J. Biol. Chem.* **270**:12065–12074.
- Balzi, E., M. Choder, W. Chen, A. Varshavsky, and A. Goffeau. 1990. Cloning and functional analysis of the arginyl-tRNA-protein transferase gene *ATE1* of *Saccharomyces cerevisiae*. *J. Biol. Chem.* **265**:7464–7471.
- Bartel, B., I. Wüning, and A. Varshavsky. 1990. The recognition component of the N-end rule pathway. *EMBO J.* **9**:3179–3189.
- Baumeister, W., J. Walz, F. Zühl, and E. Seemüller. 1998. The proteasome: paradigm of a self-compartmentalizing protease. *Cell* **92**:367–380.
- Byrd, C., G. C. Turner, and A. Varshavsky. 1998. The N-end rule pathway controls the import of peptides through degradation of a transcriptional repressor. *EMBO J.* **17**:269–277.
- Chau, V., J. W. Tobias, A. Bachmair, D. Marriotti, D. J. Ecker, D. K. Gonda, and A. Varshavsky. 1989. A multiubiquitin chain is confined to specific lysine in a targeted short-lived protein. *Science* **243**:1576–1583.
- Ciechanover, A., S. Ferber, D. Ganoth, S. Elias, A. Hershko, and S. Arfin. 1988. Purification and characterization of arginyl-tRNA-protein transferase from rabbit reticulocytes. *J. Biol. Chem.* **263**:11155–11167.
- Coux, O., K. Tanaka, and A. L. Goldberg. 1996. Structure and functions of the 20S and 26S proteasomes. *Annu. Rev. Biochem.* **65**:801–817.
- Davydov, I. V., D. Patra, and A. Varshavsky. The N-end rule pathway in *Xenopus* oocyte extracts. *Arch. Biochem. Biophys.*, in press.
- Dayal, V. K., G. Chakraborty, J. A. Sturman, and N. A. Ingolia. 1990. The site of amino acid addition to posttranslationally modified proteins in regenerating rat sciatic nerves. *Biochim. Biophys. Acta* **1038**:172–177.
- deGroot, R. J., T. Rümepf, R. J. Kuhn, and J. H. Strauss. 1991. Sindbis virus RNA polymerase is degraded by the N-end rule pathway. *Proc. Natl. Acad. Sci. USA* **88**:8967–8971.
- Du, F., and A. Varshavsky. Unpublished data.
- Ferber, S., and A. Ciechanover. 1987. Role of arginine-tRNA in protein degradation by the ubiquitin pathway. *Nature* **326**:808–811.
- Gonda, D. K., A. Bachmair, I. Wüning, J. W. Tobias, W. S. Lane, and A. Varshavsky. 1989. Universality and structure of the N-end rule. *J. Biol. Chem.* **264**:16700–16712.
- Grigoryev, S., A. E. Stewart, Y. T. Kwon, S. M. Arfin, R. A. Bradshaw, N. A. Jenkins, N. J. Copeland, and A. Varshavsky. 1996. A mouse amidase specific for N-terminal asparagine: the gene, the enzyme, and their function in the N-end rule pathway. *J. Biol. Chem.* **271**:28521–28532.
- Grigoryev, S., and A. Varshavsky. Unpublished data.
- Haas, A. J., and T. J. Siepmann. 1997. Pathways of ubiquitin conjugation. *FASEB J.* **11**:1257–1268.
- Hershko, A. 1991. The ubiquitin pathway for protein degradation. *Trends Biochem. Sci.* **16**:265–268.
- Hill, C. P., N. L. Johnston, and R. E. Cohen. 1993. Crystal structure of a ubiquitin-dependent degradation substrate: a three-disulfide form of lysozyme. *Proc. Natl. Acad. Sci. USA* **90**:4136–4140.
- Hochstrasser, M. 1996. Ubiquitin-dependent protein degradation. *Annu. Rev. Genet.* **30**:405–439.
- Hondermarck, H., J. Sy, R. A. Bradshaw, and S. M. Arfin. 1992. Dipeptide inhibitors of ubiquitin-mediated protein turnover prevent growth factor-induced neurite outgrowth in rat pheochromocytoma PC12 cells. *Biochem. Biophys. Res. Commun.* **30**:280–288.
- Ichetovkin, I. L., G. Abramochkin, and T. E. Shrader. 1997. Substrate recognition by the leucyl/phenylalanyl-tRNA protein transferase: conservation within the enzyme family and localization to the trypsin-resistant domain. *J. Biol. Chem.* **272**:33009–33014.
- Johnston, J., and A. Varshavsky. Unpublished data.
- Kajji, H., G. D. Novelli, and A. Kajji. 1963. A soluble amino acid-incorporating system from rat liver. *Biochim. Biophys. Acta* **76**:474–479.
- Kay, G. F., A. Ashworth, G. D. Penny, M. Dunlop, S. Swift, N. Brockdorff, and S. Rastan. 1991. A candidate spermatogenesis gene on the mouse Y chromosome is homologous to ubiquitin-activating enzyme E1. *Nature* **354**:486–489.
- King, R. W., R. J. Deshaies, J. M. Peters, and M. W. Kirschner. 1996. How proteolysis drives the cell cycle. *Science* **274**:1652–1659.
- Kwon, Y. T., V. Denenberg, and A. Varshavsky. Unpublished data.
- Kwon, Y. T., Y. Reiss, V. A. Fried, A. Hershko, J. K. Yoon, D. K. Gonda, P. Sangan, N. G. Copeland, N. A. Jenkins, and A. Varshavsky. 1998. The mouse and human genes encoding the recognition component of the N-end rule pathway. *Proc. Natl. Acad. Sci. USA* **95**:7898–7903.
- Kwon, Y. T., and A. Varshavsky. Unpublished data.
- Levy, F., N. Johnsson, T. Rümepf, and A. Varshavsky. 1996. Using ubiquitin to follow the metabolic fate of a protein. *Proc. Natl. Acad. Sci. USA* **93**:4907–4912.
- Li, J., and C. M. Pickart. 1995. Inactivation of arginyl-tRNA protein transferase by a bifunctional arsenoxide: identification of residues proximal to arsenoxide site. *Biochemistry* **34**:139–147.
- Li, J., and C. M. Pickart. 1995. Binding of phenylarsenoxide to Arg-tRNA-protein transferase is independent of vicinal thiols. *Biochemistry* **34**:15829–15837.
- Madura, K., R. J. Dohmen, and A. Varshavsky. 1993. N-recognition/Ubc2 interactions in the N-end rule pathway. *J. Biol. Chem.* **268**:12046–12054.
- Madura, K., and A. Varshavsky. 1994. Degradation of G α by the N-end rule pathway. *Science* **265**:1454–1458.
- Mitchell, M. J., D. R. Woods, P. K. Tucker, J. S. Opp, and C. E. Bishop. 1991. Homology of a candidate spermatogenesis gene from the mouse Y chromosome to the ubiquitin-activating enzyme E1. *Nature* **354**:483–486.
- Mumberg, G., R. Müller, and M. Funk. 1994. Regulatable promoters of *Saccharomyces cerevisiae*: comparison of transcriptional activity and their use for heterologous expression. *Nucleic Acids Res.* **22**:5767–5768.
- Murre, C., P. McCaw, and D. Baltimore. 1989. A new DNA binding and dimerization motif in immunoglobulin enhancer binding, daughterless, MyoD, and myc proteins. *Cell* **56**:777–783.
- Ota, I. M., and A. Varshavsky. 1993. A yeast protein similar to bacterial two-component regulators. *Science* **262**:566–569.
- Pickart, C. M. 1997. Targeting of substrates to the 26S proteasome. *FASEB J.* **11**:1055–1066.
- Rao, H., and A. Varshavsky. Unpublished data.
- Rechsteiner, M., L. Hoffman, and W. Dubiel. 1993. The multicatalytic and 26S proteases. *J. Biol. Chem.* **268**:6065–6068.
- Reiss, Y., and A. Hershko. 1990. Affinity purification of ubiquitin-protein ligase on immobilized protein substrates. *J. Biol. Chem.* **265**:3685–3690.
- Rothstein, R. 1991. Targeting, disruption, replacement, and allele rescue: integrative DNA transformation in yeast. *Methods Enzymol.* **194**:281–301.
- Rubin, D. M., S. van Nocker, M. Glickman, O. Coux, I. Wefes, S. Sadis, H. Fu, A. Goldberg, R. Vierstra, and D. Finley. 1997. ATPase and ubiquitin-binding proteins of the yeast proteasome. *Mol. Biol. Rep.* **24**:17–26.
- Scheffner, M., S. Smith, and S. Jentsch. 1998. The ubiquitin conjugation system, p. 65–98. *In* J.-M. Peters, J. R. Harris, and D. Finley (ed.), *Ubiquitin and the biology of the cell*. Plenum Press, New York, N.Y.
- Shrader, T. E., J. W. Tobias, and A. Varshavsky. 1993. The N-end rule in *Escherichia coli*: cloning and analysis of the leucyl, phenylalanyl-tRNA-protein transferase gene *aat*. *J. Bacteriol.* **175**:4364–4374.
- Sijst, A. J. A. M., I. Pilip, and E. G. Pamer. 1997. The *Listeria monocytogenes*-secreted p60 protein is an N-end rule substrate in the cytosol of infected cells. *J. Biol. Chem.* **272**:19261–19268.
- Soffer, R. L. 1980. Biochemistry and biology of aminoacyl-tRNA-protein transferases, p. 493–505. *In* D. Söll, J. Abelson, and P. R. Schimmel (ed.), *Transfer RNA: biological aspects*. Cold Spring Harbor Laboratory Press, Cold Spring Harbor, N.Y.
- Solomon, V., V. Baracos, P. Sarraf, and A. Goldberg. When muscles atrophy, rates of ubiquitin conjugation increase, largely through activation of the N-end rule pathway. *Proc. Natl. Acad. Sci. USA*, in press.
- Solomon, V., S. H. Lecker, and A. L. Goldberg. 1998. The N-end rule pathway mediates a major fraction of protein degradation in skeletal muscle. *J. Biol. Chem.* **273**:25216–25222.
- Stewart, A. 1995. *Trends in genetics nomenclature guide*. Elsevier Science, Ltd., Cambridge, United Kingdom.
- Stewart, A. E., S. M. Arfin, and R. A. Bradshaw. 1995. The sequence of porcine protein N-terminal asparagine amidohydrolase: a new component of the N-end rule pathway. *J. Biol. Chem.* **270**:25–28.
- Taban, C. H., H. Hondermarck, R. A. Bradshaw, and B. Boilly. 1996. Effect of a dipeptide inhibiting ubiquitin-mediated protein degradation on nerve-dependent limb regeneration in the newt. *Experientia* **52**:865–870.
- Tobias, J. W., T. E. Shrader, G. Rocap, and A. Varshavsky. 1991. The N-end rule in bacteria. *Science* **254**:1374–1377.

54. **Varshavsky, A.** 1997. The N-end rule pathway of protein degradation. *Genes Cells* 2:13–28.
55. **Varshavsky, A.** 1997. The ubiquitin system. *Trends Biochem. Sci.* 22:383–387.
56. **Varshavsky, A., C. Byrd, I. V. Davydov, R. J. Dohmen, F. Du, M. Ghislain, M. Gonzalez, S. Grigoryev, E. S. Johnson, N. Johnsson, J. A. Johnston, Y. T. Kwon, F. Lévy, O. Lomovskaya, K. Madura, I. Ota, T. Rumenapf, T. E. Shrader, T. Suzuki, G. Turner, P. R. H. Waller, and A. Webster.** 1998. The N-end rule pathway, p. 223–278. *In* J.-M. Peters, J. R. Harris, and D. Finley (ed.), *Ubiquitin and the biology of the cell*. Plenum Press, New York, N.Y.
- 56a. **Wang, H. R., and A. Varshavsky.** Unpublished data.
57. **Wang, Y. M., and N. A. Ingolia.** 1997. N-terminal arginylation of sciatic nerve and brain proteins following injury. *Neurochem. Res.* 22:1453–1459.